Ligand-field effects for the 3*p* photoelectron spectra of Cr_2O_3

Paul S. Bagus*
Department of Chemistry, University of North Texas, Denton, Texas 76203-5070, USA

Eugene S. Ilton and James R. Rustad
Pacific Northwest National Laboratory, 902 Battelle Boulevard, P.O. Box 999, Richland, Washington 99352, USA
(Received 24 December 2003; published 28 May 2004)

A major reason for the departure of core level X-ray photoelectron spectra (XPS) of transition metal cations in oxides from the predictions of atomic models is shown to arise from ligand field splittings in the initial state of photoemission. This splitting often leads to a change in the spatial degeneracy of the initial state but the consequences of this for XPS have not been explicitly identified in prior work. Further changes arise from ligand field splittings in the core-hole final states. Results are reported for non-empirical, cluster model many body wavefunctions for the 3*p* XPS of Cr_2O_3. The agreement of the theoretical cluster model XPS with experiment is considerably improved over the pure atomic model. Furthermore, the treatment allows screening of the core hole through changes in the covalent character of the cluster orbitals. This is quite different from the usual description of screening in oxides within the framework of charge transfer configurations and it offers new insights into the role of charge transfer for satellite structure.

DOI: 10.1103/PhysRevB.69.205112 PACS number(s): 79.60.−i, 61.46.+w, 82.80.Pv

I. INTRODUCTION

The relative importance of intra- and inter-atomic effects continue to pose problems for interpreting X-Ray Photoemission Spectra (XPS) of transition metal, TM, ionic crystals.[1–5] These problems need to be resolved in order to use XPS to interpret materials properties[6] including the effective oxidation state of the metal cation.[7] The many-electron atomic contributions for the 2*p*, 3*p*, and 3*s* XPS of 3*d* TM's have been studied extensively; see, e.g., Refs. 1, 5, 8, and 9. In particular, the Gupta and Sen[8] calculations for the 2*p* XPS of several TM cations have been used to model the TM oxidation state in various complexes.[10–12] However, inter-atomic effects also contribute to the XPS.[6,13–21] In this paper, we identify and establish the importance of condensed phase physical mechanisms that have not been explicitly related to XPS spectra in previous work based either on *ab initio*[4,13] or on parametrized, model Hamiltonian[14,17,18,21] cluster model studies. These mechanisms involve the ligand field splittings of the TM *d* shell and the covalent, bonding and anti-bonding, mixing of TM *d* and ligand *p* orbitals.

Of particular importance is the change in the spatial degeneracy of the initial state of the open *d* shell compound from that of the isolated TM cation due to the presence of the crystal field. We have examined this effect by studying the Cr 3*p* XPS in Cr_2O_3 using a CrO_6 cluster model. While the Cr^{3+} $3d^3$ cation has a ^4F initial state with a 7 fold spatial degeneracy, this spatial degeneracy is removed in the presence of the crystal field and the initial state of CrO_6 is the spatially nondegenerate $^4A_2$. The crystal field splitting of the *d*-levels is well known.[22] Semi-empirical cluster model studies of the XPS of TM complexes have included parameters to represent this crystal field splitting;[2(a),17,18,21] one of these studies[21] was for the Cr 2*p* and 3*p* XPS of Cr_2O_3. However, to our knowledge, the direct connection of the lowering of the spatial degeneracy of the TM cation to the character of the XPS spectra has not been addressed previously. In an earlier study[5] of atomic many-body effects for Cr^{3+}, we showed that the spatial degeneracy of the initial state yielded a complex and rich 3*p* XPS spectrum that had significant deviations from the XPS observed for α-Cr_2O_3. In this paper, we present results for a strictly *ab initio* treatment of an embedded CrO_6 cluster model of α-Cr_2O_3 that reduces this complexity, especially for the low binding energy, BE, region of the spectra and improves agreement of the theory with experiment. In particular, we show that the $^4A_2$ ligand field split initial state is a major, perhaps the dominant, condensed phase effect on the XPS of Cr 3*p* for α-Cr_2O_3.

A second novel feature of the present work relates to the role of charge transfer, CT, especially as it contributes to the XPS satellite structure. This CT from ligands to the TM *d* shell is a key inter-atomic effect for the core–hole final states. It is often described in terms of configurations where there is no CT, d^n, or where there is full CT, $d^{n+1}\underline{L}$, where $\underline{L}$ indicates a ligand hole.[6,17–21] The final, core–hole, state WF's are written as mixtures of d^n and $d^{n+1}\underline{L}$ configurations;[13–15,17,18,21] although, in extreme cases, the final states are considered to be entirely d^n or $d^{n+1}\underline{L}$.[19,20] In this theoretical formulation, the *d* orbital is considered as a pure metal orbital and the *L* is considered as a pure ligand hole. In fact, the dominantly *d* and the dominantly ligand orbitals are not pure but are mixtures with a bonding and anti-bonding character.[22,23] For our *ab initio* 3*p*-hole state CrO_6 cluster WF's, we find that this mixing is considerably different for the initial and final state WF's. Although we do find a large O(2*p*) to Cr(3*d*) CT for the core–hole states, the increase in the number of Cr(3*d*) electrons arises largely because of changes in the composition of closed shell, dominantly O(2*p*), orbitals. Thus, this CT may not contribute to low lying satellites as it does in the usual model based on d^n and $d^{n+1}\underline{L}$ configurations.

Key computational, methodological, and theoretical aspects of our work are discussed in the following section, Sec.

II. The theoretical and experimental results for the Cr $3p$ XPS are compared and discussed in Sec. III and our conclusions are summarized in Sec. IV.

II. THEORETICAL AND COMPUTATIONAL CONSIDERATIONS

Our materials model for Cr_2O_3 is an embedded CrO_6 cluster with -2 (anion) and $+3$ (cation) point charges (PC's) placed at 429 lattice sites within a 10 Å radius of the central Cr atom. The atoms and PC's have the corundum crystal structure.[24] Although, due to covalent bonding, the Madelung potential is less for the real crystal than for the cluster model, the use of formal charges is not expected to introduce artifacts. The charge on the cluster is -9, consistent with the nominal ionicities. The symmetry of the embedded cluster is C_3 and it is distorted from cubic, O_h, symmetry. Since these distortions are relatively minor, we use the simpler nomenclature for O_h when we describe the cluster WF's.

The CrO_6 orbitals were obtained by solution of Hartree–Fock (HF) equations for the average of configurations for initial, $3p^6 3d^3$, and $3p$-hole final, $3p^5 3d^3$, configurations;[1,5] the cluster $3d$ orbitals are split into t_{2g} and e_g and they are anti-bonding combinations of Cr($3d$) and O($2p$).[23,24] With these orbitals, configuration interaction (CI) WF's were determined for all distributions of the open shell electrons within the open shell spaces;[1,5] for the $3p$-hole WF's, only configurations with 5 electrons in the $3p$ orbitals were included in the CI WF's. For the CrO_6 initial state, we also optimized the orbitals for the HF WF of the ground $^4A_2$ multiplet. The overlap of this HF WF with the CI WF for the average of configuration orbitals is 0.998 showing that the approximation of using averaged orbitals is highly accurate. These complete open shell CI WF's include the many body effects arising from angular momentum coupling and recoupling within the open shells.[1,5,25] The selection rule is that XPS transitions are allowed only to $3p$-hole configurations where the open d shell is $t_{2g}^3(^4A_2)$ as in the initial state. The $3p^5$, or t_{1u}^5, couples to $^2T_1$ and the XPS allowed $3p$-hole final states are either $^5T_2$ or $^3T_2$ multiplets. Within the p^5d^3 manifold, there are 4 $^5T_2$ and 19 $^3T_2$ configurations but only one of each spin is allowed. However, the allowed configurations can mix into all of the 4 $^5T_2$ or all of the 19 $^3T_2$ final state CI WF's. The relative intensities, I_{rel}, are obtained from the initial state and final state CI WF's with the Sudden Approximation (SA) modified by the final state multiplicities, 3 or 5.[3,26]

III. DISCUSSION

Figures 1 and 2 compare nonrelativistic theoretical $3p$ XPS for free Cr^{3+} and the CrO_6 cluster with experiment for α-Cr_2O_3; see Ilton *et al.*[5] for experimental details. In order to compare theory with experiment, the SA I_{rel} are broadened with a mixed 50% Gaussian–50% Lorentzian to yield a net 1.1 eV full width at half maximum and the positions of the peaks are rigidly shifted by a constant energy to obtain the best match with the experimental XPS. In the figures, we show the broadened contributions from individual final ionic states or, when the states are close together, from closely spaced groups of final ionic states. In addition, a full theoretical curve that shows the sum of these individual contributions is also given.

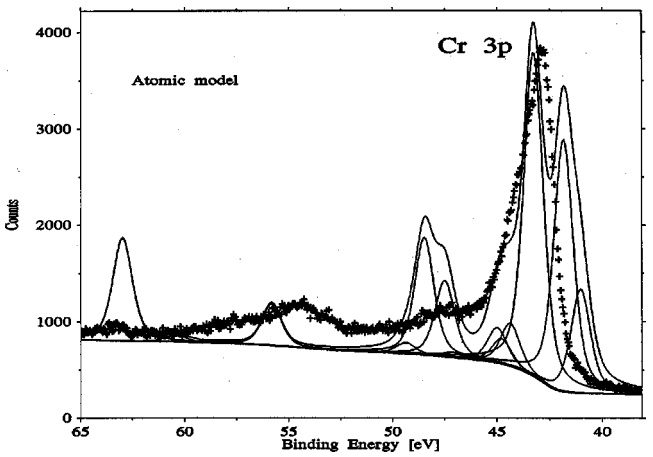

FIG. 1. A comparison of XPS from theory (smooth lines) for free Cr^{3+} with experiment for Cr_2O_3. Lifetime and instrumental broadening are included in the theoretical XPS spectra. The broadened contributions for individual final states or for closely spaced groups of final states are shown and the full theoretical envelope represents the sum of the individual contributions.

The nonrelativistic and fully relativistic results for free Cr^{3+} are very similar;[5] relativistic effects should also be minor for the $3p$ XPS of CrO_6. However, the free Cr^{3+} and the embedded CrO_6 XPS are very different, where the cluster model is more consistent with experiment for Cr_2O_3, especially in the region near the leading edge of the Cr $3p$ XPS. It is clear from Fig. 1 that the free Cr^{3+} ion does not yield a good approximation to the experimental XPS in this region. The full theoretical envelope has a pronounced doublet with a splitting of $\sim$1.5 eV at the leading edge. This is not at all consistent with experiment and it is not possible to align this doublet in a unique way with the leading edge of the experi-

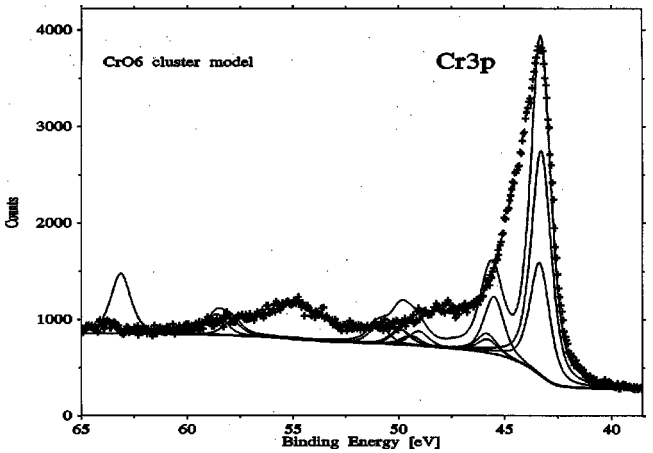

FIG. 2. A comparison of XPS from theory (smooth lines) for embedded CrO_6 with experiment for Cr_2O_3; see the caption to Fig. 1.

TABLE I. Theoretical relative energies, E_{rel} in eV, for high spin, quartet, multiplets of free Cr^{3+} and embedded CrO_6.

Cr^{3+}		CrO_6	
	E_{rel}		E_{rel}[a]
^4F	0	$^4A_2$	0
^4P	2.16	$^4T_2$	1.83
		$^4T_1$	2.85–2.86
		$^4T_1$	4.54–4.55

[a]The energy ranges for the ^4T multiplets indicate the small deviations from O_h symmetry.

mental spectrum. The major contribution to this doublet comes from different orbital angular momentum couplings of the d-shell $3d^3(^4F)$ with the core–hole $3p^5(^2P)$; the significance of this angular momentum coupling for the atom will be considered below. On the other hand, the CrO_6 embedded cluster model of Cr_2O_3 yields a theoretical $3p$ XPS that is more consistent with experiment. For both theory and experiment, there is a dominant main peak and a lower intensity satellite at ~ 2 eV relative to the main peak; although the agreement of theory and experiment is not perfect, the use of the cluster model gives a major improvement. We consider the physical reasons that the ligand field splitting leads to these large changes in the XPS.

In Table I, we illustrate the ligand and crystal field effects on energies and degeneracies by showing the calculated E_{rel} for the high spin, initial state multiplets of both Cr^{3+} and CrO_6. The crystal field of Cr_2O_3 splits ^4F into $^4A_2$, $^4T_2$, and $^4T_1$ multiplets while ^4P goes to $^4T_1$.[23] The combination of crystal and ligand field effects that lift the degeneracy of the ^4F multiplet are comparable to the atomic angular momentum couplings[27] that split the ^4F and ^4P multiplets.[28] The quartet multiplets shown in Table I are the only initial state couplings that can lead to high spin coupled, quintet, $3p$-hole final configurations.[1,3,5] We examine these quintet states in detail to understand how the ligand field splitting dramatically changes the XPS.

For free Cr^{3+}, the $3p$ XPS allowed high spin final state multiplets are ^5G, ^5F, and ^5D arising from the angular momentum coupling of $3p^5(^2P)$ and $3d^3(^4F)$.[5,27] In addition, there is an XPS forbidden ^5D multiplet arising from $3p^5(^2P)3d^3(^4P)$; the allowed and forbidden ^5D configurations mix to form the final state WF's, $^5D_1$ and $^5D_2$, and the XPS intensity to the allowed ^5D multiplet is shared between these two final states. In Table II, we give the E_{rel} and XPS I_{rel} for these four high spin $3p$-hole multiplets. The I_{rel} for the allowed ^5G, ^5F, and ^5D multiplets are, to a good approximation, proportional to the statistical weights of the multiplets, $(2S+1)\times(2L+1)$.[29,30] Thus, see Table II, $I_{rel}(^5G):I_{rel}(^5F):I_{rel}(^5D_1)+I_{rel}(^5D_2)$ is 9:7:5 with the ^5G multiplet carrying the largest intensity. In sharp contrast, for CrO_6, there is only one allowed high spin final state multiplet, $^5T_2$, arising from the coupling of $3p^5(^2T_{1u})$ with $t_{2g}^3(^4A_2)$.[23] This multiplet[29] is the linear combination of the XPS allowed ^5G, ^5F, and ^5D multiplets that carries all the intensity when the initial $3d^3$ state is coupled to $^4A_2$.

TABLE II. Energies, E_{rel} in eV, and intensities, I_{rel}, for the $3p$ XPS of Cr^{3+} and CrO_6; $E_{rel}=0$ and $I_{rel}=1$ for the lowest $3p$-hole state.

Cr^{3+}			CrO_6		
	E_{rel}	I_{rel}		E_{rel}[a]	I_{rel}
$^5D_1$	0	1	$^5T_2(a)$	0–0.07	1
^5F	0.81	2.42	$^5T_2(b)$	2.54–2.56	0.04
^5G	2.33	3.11	$^5T_2(c)$	2.57–2.59	0.06
$^5D_2$	6.43	0.73	$^5T_2(d)$	6.58–6.62	0.04

[a]See the footnote to Table I.

There are three XPS forbidden $^5T_2$ multiplets[23] that arise from the coupling of $3p^5(^2T_{1u})$ with $t_{2g}^2(^3T_1)e_g^1(^2E);^4T_1$, $t_{2g}^2(^3T_1)e_g^1(^2E);^4T_2$, and $t_{2g}^1(^2T_2)e_g^2(^3A_2);^4T_1$. These four $^5T_2$ configurations mix to form the $3p$-hole WF's denoted $^5T_2(a)$ to $^5T_2(d)$ whose E_{rel} and I_{rel} are given in Table II. The XPS allowed configuration is the dominant contribution to the first final state and only 12% of the intensity is lost to the other final states. It is clear that reducing the symmetry of the initial state from the spatially degenerate ^4F for free Cr^{3+} to the spatially nondegenerate $^4A_2$ for CrO_6 dramatically reduces the complexity of the high spin coupled XPS peaks and, for CrO_6, a single final state dominates the $3p$ XPS.

For the low spin coupled $3p$-hole states, the XPS allowed configuration; $3p^5(^2T_1)$ coupled with $t_{2g}^3(^4A_2)$ to $^3T_2$, is exchange split from the allowed $^5T_2$ configuration by $4\,\overline{K}(3p,t_{2g})\approx 10$ eV, where $\overline{K}$ is an average exchange integral between the $3p$ and t_{2g} orbitals.[23,27] However, in contrast to the high spin final states where the intensity goes dominantly to a single multiplet, for the low spin states, it is distributed into several $^3T_2$ states over a range of 20 eV. The largest $^3T_2$ I_{rel} is to multiplets at $E_{rel}=2.2$ and 19.9 eV, where $E_{rel}=0$ is the lowest $^5T_2$ state. The XPS allowed $^3T_2$ configuration has a weight of $\sim 25\%$ in each of these two states; the remaining 50% of the weight is distributed over several other $^3T_2$ multiplets and its weight for any individual multiplet is less than 10%. Thus, the allowed low spin configuration is not the dominant term in any final state. For the $3p$ XPS of several free TM cations,[25] it has also been found that the allowed low spin $3p$-hole configurations were distributed over several multiplets; however, the mixing was not as extreme as that found for CrO_6. Furthermore, the low spin contributions to the XPS are quite different between free Cr^{3+} and the CrO_6 model of Cr_2O_3; see Figs. 1 and 2, and Table II to separate the high and low spin contributions. These differences arise: (1) From the different XPS selection rules for the spatially degenerate $3d^3(^4F)$ initial state of free Cr^{3+} and for the spatially nondegenerate $t_{2g}^3(^4A_{2g})$ initial state of CrO_6, and (2) from the ligand field splittings of the $3p$-hole configurations.

Overall, Fig. 2 shows that there is reasonable agreement between the theoretical XPS for CrO_6 and experiment. The general problem is that the higher theoretical peaks are at too high E_{rel} by $\sim 1-3$ eV. Thus, instead of the experimental shoulder at $E_{rel}\sim 1.3$ eV, theory gives a satellite at E_{rel}

TABLE III. Projected number of Cr $3d$ electrons, N_d(Proj), in the initial and lowest $3p$-hole final state WF's of CrO_6.

	Initial	Lowest $3p$-hole
Open Shell t_{2g} and e_g	2.84	2.75
Total	3.46	4.18

$\sim$2.5 eV; the theoretical peaks at $E_{\rm rel}\sim$7.5 and 15 eV can be assigned to observed peaks at $E_{\rm rel}\sim$5 and $\sim$12 eV, respectively. However, it is difficult to reconcile the theoretical peak at $E_{\rm rel}\sim$20 eV with any of the observed features. In Ref. 21, an *ad hoc* energy dependent lifetime parameter for the $3p$-hole peaks is used to broaden the intensity of the calculated peak at $E_{\rm rel}\sim$20 eV. The physical basis for this approach needs to be tested by extending our nonempirical CI model to include additional many-body effects and an improved treatment of the condensed phase.

At this point, we consider the nature of the final state core-hole screening as shown by the character of the CrO_6 WF's. This screening is included in our treatment of CrO_6 through covalent mixing, primarily, of the ligand O($2p$) and the Cr t_{2g} and e_g $3d$ orbitals. The fully occupied t_{2g} and e_g, dominantly ligand, orbitals have bonding character while the partially occupied orbitals are dominantly Cr $3d$ and have anti-bonding character.[22,23] The number of Cr $3d$ electrons in the cluster WF's, N_d(Proj), is obtained as the expectation value of a projection operator.[31] In Table III, we give N_d(Proj) for the initial, $^4A_2$, and for the lowest $3p$-hole final state of CrO_6; the contribution to N_d(Proj) from the open shell, dominantly Cr $3d$, t_{2g} and e_g, orbitals is also given. For the initial state, the decrease of N_d(Proj) for the t_{2g}^3 orbitals from the nominal value of 3 indicates a modest, $\sim$5%, ligand character in these orbitals. The total count of d electrons N_d(Proj)$=3.46$ arises because of the bonding character of the filled, dominantly ligand, orbitals of both t_{2g} and e_g symmetry. For the lowest $3p$-hole state, the hole on Cr is screened by a substantial increase in the bonding character of the ligand orbitals. This leads to a total number of 4.2 Cr $3d$ electrons, an increase of 0.7 from the ground state where there is no $3p$ hole. Although there is a large CT to the Cr($3d$) that screens the $3p$ core-hole and although the occupation of the Cr $3d$ orbital in the WF's for the final, core-hole states is $\sim$4 electrons, it is misleading to describe the WF's with this CT as dominated by a $d^4\underline{L}$ configuration. The CT in our CI WF's arises from covalent mixings of the d and ligand orbitals to form orbitals with bonding and anti-bonding character. As expected from the orientations of the t_{2g} and e_g d orbitals,[23] the covalent mixings are larger for e_g than for t_{2g} symmetries. Thus the dominantly Cr $3d$ e_g have a larger anti-bonding character and hence a smaller d count than the $3d$ t_{2g} orbitals. The lowest $3p$-hole state is dominantly t_{2g}^3 while the higher energy states have more e_g character. Hence the N_d value is somewhat, but not dramatically, lower for these states.

The overall effect of this screening by increasing the covalent character of the cluster orbitals is to reduce the SA $I_{\rm rel}$ by similar amounts for all the states included in our many-body CI treatment. The intensity lost from these states appears in shake-up and shake-off states[3,32,33] that we have not included in our model. Many of these states have very large $E_{\rm rel}$;[32] others may be more low-lying.[33] Our treatment of the core-hole screening is quite different from the semi-empirical approach taken in Ref. 21 for cluster models of Cr_2O_3 where this final state screening is modeled by the CI mixing of non-CT, d^3, and CT, $d^4\underline{L}$, configurations. From Table III, it is clear that the covalent mixing of Cr $3d$ with ligand orbitals for the $3p$-hole states leads to a large CT screening of the Cr $3p$-hole. It is worth stressing that screening by $d^{n+1}\underline{L}$ configurations introduces different physics than when the screening arises because the covalency of the orbitals is changed. The open shell structure and, hence, the spin and angular momentum couplings of the dominantly d-shells are not changed dramatically when the degree of covalency is changed. This is especially true when the changes in the character of the open shell orbitals are relatively modest; in this case the main changes are for the d-shell Coulomb and exchange integrals that will have somewhat different values. On the other hand, the change in the number of d electrons when the screening is due to CT with the configuration $d^{n+1}\underline{L}$ must lead to substantially different spin and orbital angular momentum coupling of the d shell electrons. We point out in the Concluding Remarks, where we review prior results for the $3s$ XPS of NiO, that these two types of final state screening may both be present in a given system.

IV. CONCLUDING REMARKS

The present study provides substantial insight into the physical origins of the Cr_2O_3 $3p$ XPS. In particular, the removal of the spatial degeneracy of the ^3F initial state of the isolated Cr^{3+} $3d^3$ cation to a nondegenerate $^3A_2$ initial state in the crystalline environment leads to major changes in the Cr $3p$ XPS. We note that the ligand field splitting of the d levels will not cause a change in the degeneracy in the case of Mn^{2+} where the isolated ion is a nondegenerate ^6S multiplet and the ligand field splitting changes this to $^6A_{1g}$, also nondegenerate. This may explain, at least in part, why the effect of the crystalline environment is not especially large for the Mn $2p$ and $3p$ XPS in MnO.[2(a)] Also, when the core hole is in an s-shell, changes in the spatial angular coupling of the open d shell caused by the ligand field are not important because the core-hole is totally symmetric. However for $3p$-holes in other TM's, the change of the d^n degeneracy in the initial state, induced by the ligand field splitting is likely to lead to important changes in the XPS.

Furthermore, our work shows that ligand screening of the core hole on the Cr cation due to changes in the covalent mixing between the Cr $3d$ and the ligand $2p$ is quite significant. The reasonable agreement of our theoretical Cr $3p$ XPS for the embedded CrO_6 cluster with experiment suggests that the shake satellites due to this screening may be at higher energies than normally examined in the XPS experiments. However, a calculation where configurations to represent these shake states are included is required in order to fully

support this supposition. It is appropriate to ask about the generality of the importance of the screening of core-holes by the covalent mixing of TM d and ligand $2p$ orbitals. Because there is only very limited theoretical information available, a detailed comparison of the character of the core-hole screening among different TM oxides cannot be made. However, a partial and limited comparison of the screening for Cr_2O_3, described in this paper, with the screening for NiO, described in previous papers[13,34] on embedded NiO_6 cluster models, is possible. Although our Cr_2O_3 results are for the screening of the TM $3p$-hole and the earlier NiO results are for the screening of the TM $3s$-hole, the comparison is meaningful since both the Cr $3p$ and Ni $3s$ are core orbitals. For NiO, the total number of d electrons, as given by projection[31] on HF WF's for the initial state and the lowest $3s$-hole states, is $N_d(\mathrm{Proj})=8.13$ and 8.32 for the initial and $3s$-hole states, respectively. Recall that for Ni^{2+}, in ionic materials, the nominal number of d electrons is 8 and the d configuration is $3d^8$. Thus, the values of $N_d(\mathrm{Proj})$ show a very different covalent character for Ni than for Cr; see Table III. In particular, for Cr, the covalent screening of the core-hole increases the number of electrons in the $3d$ shell by 0.7, while for Ni, this screening only increases the number of $3d$ electrons by 0.2 electrons. On the other hand, for NiO, the mixing of d^8 and $d^9\underline{L}$ $3s$-hole configurations makes major contributions to the XPS and a meaningful interpretation of the Ni $3s$ XPS of NiO cannot be made unless this mixing is taken into account.[13,34] Unfortunately, we do not have *ab initio* results regarding the equivalent d^3 and $d^4\underline{L}$ mixing for the $3p$-hole states of Cr_2O_3. However, this limited comparison of the final state screening for Cr_2O_3 and NiO indicates that the character of the screening and, possibly, the consequences of this screening for the XPS may depend strongly on the specific system. A systematic study comparing the screening in a range of TM ionic systems would permit the relative importance of screening through changes in the covalent character and through mixing of d^n and $d^{n+1}\underline{L}$ configurations to be established; it would also clarify the extent of the differences as well as the complimentary character of these two mechanisms

Thus, the results that we have presented based on the first, strictly fully nonempirical cluster study of TM $3p$ XPS in an ionic solid have allowed us to draw new and important conclusions for the interpretation of XPS experiments. These considerations need to be taken into account in order to correctly relate features of the $3p$ XPS to the chemistry and chemical bonding of TM complexes.

ACKNOWLEDGMENTS

P.S.B. acknowledges partial support from the Pacific Northwest National Laboratory. The computational support provided by the National Center for Supercomputing Applications, Urbana—Champaign, Illinois is also acknowledged. E.S.I. and J.R.R. acknowledge support from the Geosciences Research Program, Office of Basic Energy Sciences, U.S. Department of Energy (DOE). A portion of the research was performed at the W. R. Wiley Environmental Molecular Sciences Laboratory, a national scientific user facility sponsored by the U.S. DOE and located at PNNL, operated for the DOE by Battelle.

*Electronic address: bagus@unt.edu

[1] P. S. Bagus, R. Broer, W. A. de Jong, W. C. Nieuwpoort, F. Parmigiani, and L. Sangaletti, Phys. Rev. Lett. **84**, 2259 (2000).
[2] (a) M. Taguchi, T. Uozumi, K. Okada, H. Ogasawara, and A. Kotani, Phys. Rev. Lett. **86**, 3692 (2001); (b) Paul S. Bagus, R. Broer, W. A. de Jong, W. C. Nieuwpoort, F. Parmigiani, and L. Sangaletti, *ibid.* **86**, 3693 (2001).
[3] L. Sangaletti, F. Parmigiani, and P. S. Bagus, Phys. Rev. B **66**, 115106 (2002).
[4] A. H. de Vries, L. Hozoi, R. Broer, and P. S. Bagus, Phys. Rev. B **66**, 035108 (2002).
[5] E. S. Ilton, W. A. deJong, and P. S. Bagus, Phys. Rev. B **68**, 125106 (2003).
[6] (a) G. van der Laan, C. Westra, C. Haas, and G. A. Sawatzky, Phys. Rev. B **23**, 4369 (1981); (b) J. Zaanen, C. Westra, and G. A. Sawatzky, *ibid.* **33**, 8060 (1986).
[7] S. A. Chambers and T. Droubay, Phys. Rev. B **64**, 075410 (2001).
[8] R. P. Gupta and S. K. Sen, Phys. Rev. B **10**, 71 (1974); **12**, 15 (1975).
[9] E. K. Vinikka and Y. Ohrn, Phys. Rev. B **11**, 4168 (1975).
[10] D. Banerjee and H. W. Nesbitt, Geochim. Cosmochim. Acta **63**, 3025 (1999).
[11] A. R. Pratt and N. S. McIntyre, Surf. Interface Anal. **24**, 529 (1996).
[12] R. M. Weaver, M. F. Hochella, and E. Ilton, Geochim. Cosmochim. Acta **66**, 4119 (2002).
[13] P. S. Bagus, G. Pacchioni, and F. Parmigiani, Chem. Phys. Lett. **207**, 569 (1993).
[14] L. Sangaletti, L. E. Depero, P. S. Bagus, and F. Parmigiani, Chem. Phys. Lett. **245**, 463 (1995).
[15] P. S. Bagus, H. J. Freund, T. Minerva, G. Pacchioni, and F. Parmigiani, Chem. Phys. Lett. **251**, 90 (1996).
[16] F. Parmigiani and L. Sangaletti, J. Electron Spectrosc. Relat. Phenom. **98-99**, 287 (1999).
[17] K. Okada and A. Kotani, J. Phys. Soc. Jpn. **61**, 4619 (1992); **60**, 772 (1991).
[18] M. Taguchi, T. Uozumi, and A. Kotani, J. Phys. Soc. Jpn. **66**, 247 (1997).
[19] V. Kinsinger, I. Sunder, P. Steiner, R. Zimmerman, and S. Huffner, Solid State Commun. **73**, 527 (1990).
[20] B. M. Veal and A. P. Pauilikas, Phys. Rev. Lett. **51**, 1995 (1983).
[21] T. Uozumi, K. Okada, and A. Kotani, J. Electron Spectrosc. Relat. Phenom. **78**, 103 (1996).
[22] J. S. Griffith, *The Theory of Transition-Metal Ions* (Cambridge University Press, Cambridge, 1971).
[23] P. S. Bagus, F. Illas, C. Sousa, and G. Pacchioni, in *Electronic Properties of Solids Using Cluster Methods*, edited by T. A. Kaplan and S. D. Mahanti (Plenum, New York, 1995), p. 93.
[24] R. W. G. Wyckoff, *Crystal Structures* (Wiley, New York, 1963).
[25] A. J. Freeman, P. S. Bagus, and J. V. Mallow, Int. J. Magn. **4**, 35 (1973).
[26] T. Åberg, Phys. Rev. **156**, 142 (1967); P. S. Bagus *et al.*, Phys. Rev. A **9**, 1090 (1974).

[27] J. C. Slater, *Quantum Theory of Atomic Structure* (McGraw-Hill, NY, 1960), Vol. II.

[28] For free Cr^{3+}, the calculated $E_{rel}(^4P)$ is ~ 0.5 eV smaller than experiment; see URL http://physics.nist.gov/cgi-bin/AtData/main_asd. This is because detailed electron correlation effects, see K. Pierloot, E. Tsokos, and B. O. Roos, Chem. Phys. Lett. **214**, 583 (1993), are not included in our CI WF's. Roughly similar correlation errors in E_{rel} are expected for the $3p$-hole XPS final states.

[29] P. A. Cox, S. Evans, and A. F. Orchard, Chem. Phys. Lett. **13**, 386 (1972).

[30] P. S. Bagus, J. L. Freeouf, and D. E. Eastman, Phys. Rev. B **15**, 3661 (1977).

[31] C. J. Nelin, P. S. Bagus, and M. R. Philpott, J. Chem. Phys. **87**, 2170 (1987).

[32] R. Manne and T. Åberg, Chem. Phys. Lett. **7**, 282 (1970).

[33] H.-J. Freund and E. W. Plummer, Phys. Rev. B **23**, 4859 (1981).

[34] P. S. Bagus, R. Broer, C. de Graff, and W. C. Nieuwpoort, J. Electron Spectrosc. Relat. Phenom. **98-99**, 303 (1999).